PHYSICAL REVIEW D **90,** 054009 (2014)

Interpreting $Z_c(3900)$ and $Z_c(4025)/Z_c(4020)$ as charged tetraquark states

Chengrong Deng,[1,†] Jialun Ping,[2,*] Hongxia Huang,[2,‡] and Fan Wang[3,§]

[1]*School of Mathematics and Physics, Chongqing Jiaotong University, Chongqing 400074, People's Republic of China*

[2]*Department of Physics, Nanjing Normal University, Nanjing 210097, People's Republic of China*

[3]*Department of Physics, Nanjing University, Nanjing 210093, People's Republic of China*

(Received 3 March 2014; published 10 September 2014)

In the framework of the color flux-tube model with a four-body confinement potential, the lowest charged tetraquark states $[Qq][\bar{Q}'\bar{q}'](Q = c, b, q = u, d, s)$ are studied by using the variational method, the Gaussian expansion method. The results indicate that some compact resonance states with three-dimensional spatial structures can be formed. These states cannot decay into two color singlet mesons $Q\bar{q}'$ and $\bar{Q}'q$ through the breakdown and recombination of color flux tubes but into $Q\bar{Q}'$ and $q\bar{q}'$. The four-body confinement potential is a crucial dynamical mechanism for the formation of these compact resonance states. The decay process is similar to that of a compound nucleus but due to the multibody color confinement. The newly observed charged states $Z_c(3900)$ and $Z_c(4025)/Z_c(4020)$ can be interpreted as the S-wave tetraquark states $[cu][\bar{c}\,\bar{d}]$ with quantum numbers $IJ^P = 11^+$ and 12^+, respectively.

DOI: 10.1103/PhysRevD.90.054009 PACS numbers: 14.20.Pt, 12.40.-y

I. INTRODUCTION

In the past decade many charmonium and bottomonium (or charmoniumlike and bottomoniumlike) states, denoted by X and Y particles, have been observed in different experiments [1]. Some of these states cannot be well accommodated in the $Q\bar{Q}$ quark model scheme. They have been interpreted as exotic hadron states [1], such as loose meson-meson molecules, compact tetraquark states, hybrid quarkonia, and baryonia or hexaquark states $q^3\bar{q}^3$. The existence of exotic hadron states has been further strengthened by the observation of the charged Z particles [2,3], because their minimum quark contents must go beyond the conventional $Q\bar{Q}$ scheme. Very recently, the BESIII Collaboration studied the process $e^+e^- \to \pi^+\pi^- J/\Psi$ at a center-of-mass energy of 4.26 GeV and observed a new charged charmoniumlike structure in the $\pi^\pm J/\Psi$ invariant spectrum, which is called $Z_c(3900)$ and has a mass of $3899.0 \pm 3.6 \pm 4.9$ MeV and a width of $46 \pm 10 \pm 20$ MeV [4]. Almost at the same time, the Belle Collaboration observed a $Z(3895)^\pm$ state with a mass of $3894.5 \pm 6.6 \pm 4.5$ MeV and a width of $63 \pm 24 \pm 26$ MeV in the $\pi^\pm J/\Psi$ invariant mass spectrum, in the process $Y(4260) \to \pi^+\pi^- J/\Psi$ [5]. The state $Z_c(3900)$ has been further confirmed by the CLEO-c Collaboration in the decay $\psi(4160) \to \pi^+\pi^- J/\Psi$ with a mass of $3886 \pm 4 \pm 2$ MeV and a width of $37 \pm 4 \pm 8$ MeV [6]. The states $Z_c(3900)$ and $Z(3895)^\pm$ have been observed by the BESIII and Belle Collaborations independently, and their masses and widths agree with each other within errors, which indicates $Z_c(3900)$ and $Z(3895)^\pm$ might be the same state [7]. Subsequently, the BESIII Collaboration studied the process $e^+e^- \to \pi^\pm(D^*\bar{D}^*)^\pm$ at a center-of-mass energy of 4.26 GeV and reported a new charged charmoniumlike structure, named $Z_c^\pm(4025)$, with a mass of $4026.3 \pm 2.6 \pm 3.7$ MeV and a width of $24.8 \pm 5.6 \pm 7.7$ MeV [8]. In addition, the BESIII Collaboration also observed another charged state $Z_c(4020)$ very close to the $(D^*\bar{D}^*)^\pm$ threshold with a mass of $4022.9 \pm 0.8 \pm 2.7$ MeV and a width of $2.9 \pm 2.7 \pm 2.6$ MeV in the $\pi^\pm h_c$ invariant mass spectrum [9].

Obviously, such charged states challenge the theoretical description of meson states as $Q\bar{Q}$ and favor tetraquark systems. A better understanding of the internal structure of these and similar resonances may provide new insights to the strong dynamics of multiquark systems and low-energy QCD. As a consequence, intense theoretical attentions have been paid to the internal structure of these charged states. So far, the theoretical interpretations can be classified into three categories. The first one is the meson-meson molecule [10], two mesons are separated at distance larger than the typical size of the mesons. The interaction between two mesons is due to the exchange of the meson and gluon, which is similar to nuclear force. Generally the interaction is weak and the mass of the state is close to the threshold of two mesons. The second one is the tetraquark states, where the four quarks may be divided into two clusters and form relatively tightly bound diquarks $[Qq]$ and antidiquarks $[\bar{Q}'\bar{q}']$, which interact through the color force due to gluon exchange or the flavor-dependent force due to meson exchange and decay through the rearrangement of the color structure [11]. The last one is hadro-quarkonium,

*Corresponding author.
jlping@njnu.edu.cn
†crdeng@cqjtu.edu.cn
‡hxhuang@njnu.edu.cn
§fgwang@chenwang.nju.edu.cn

where the heavy $Q\bar{Q}'$ pair forms a tightly bound system similar to the heavy quarkonium states. It is embedded in a light meson cloud and interacts with it by color Van der Waals force [12,13]. Which one is the true picture of these charged states? More experimental and theoretical works are needed.

The present work attempts to explore the properties of the charged tetraquark states with quark contents $[Qq][\bar{Q}'\bar{q}']$ $(Q = c, b, q = u, d, s)$ from the perspective of a phenomenological model, a color flux-tube model, using the high-precision variational method, the Gaussian expansion method (GEM). In this model, the color confinement used is not the usual two-body interaction proportional to a color charge $\lambda_i^c \cdot \lambda_j^c$ but a multibody one, which is based on lattice QCD results and has been successfully applied to study multiquark systems [14–18]. The calculation indicates that some compact tetraquark states can be formed, in which the four-body confinement potential plays a critical role, and the states cannot decay into two color singlet mesons $Q\bar{q}'$ and $\bar{Q}'q$ through the strong interaction but into $Q\bar{Q}'$ and $q\bar{q}'$ through the breakdown and rearrangement of color flux tubes. The newly observed charged states $Z_c(3900)$ and $Z_c(4025)/Z_c(4020)$ can be interpreted as the S-wave tetraquark states $[cu][\bar{c}\,\bar{d}]$ or $[cd][\bar{c}\,\bar{u}]$ with quantum numbers $IJ^P = 11^+$ and 12^+, respectively, in the color flux-tube model.

This paper is organized as follows: the color flux-tube model and the corresponding Hamiltonian are given in Sec. II. Section III is devoted to the construction of the wave functions of tetraquark states. The numerical results and discussions of the charged tetraquark states are presented in Sec. IV. A brief summary is given in the last section.

II. COLOR FLUX-TUBE MODEL AND HAMILTONIAN

Quantum chromodynamics (QCD) is nowadays widely accepted as the fundamental theory to describe hadrons and their interactions. Up to now, QCD can be evaluated systematically only in a perturbation expansion. With respect to hadrons and hadron-hadron interactions, such an expansion is invalid because the quark and gluon coupling constant varies from weak to strong. Lattice QCD (LQCD) is the most promising nonperturbative method but so time consuming that phenomenological constituent quark models (CQM) based on QCD have therefore been used extensively, such as Isgur-Karl model and chiral quark model [19,20]. CQM is formulated under the assumption that the hadrons are color singlet nonrelativistic bound states of constituent quarks with phenomenological effective masses and interactions. The effective interactions includes one-gluon-exchange (OGE), one boson exchange (OBE) and a confinement potential. The confinement potential is phenomenologically described as the sum of two-body interactions proportional to the color charges and r_{ij}^k,

$$V^C = -a_c \sum_{i>j}^{n} \lambda_i \cdot \lambda_j r_{ij}^k, \tag{1}$$

where r_{ij} is the distance between two interacting quarks q_i and q_j and k usually takes 1 or 2. An objection could be that although these models are successful phenomenologically in ordinary hadrons (q^3 baryon and $q\bar{q}$ meson), their generalization to the case of multiquarks is rather arbitrary. Furthermore, the traditional models lead to power law Van der Waals forces between color-singlet hadrons and the anticonfinement in a color symmetrical quark or antiquark pair [21,22]. The problems are related to the fact that the traditional CQM do not respect local color gauge invariance [23].

LQCD deals with the confinement phenomenon in a nonperturbative framework and its calculations on $q\bar{q}$, qqq, tetraquark and pentaquark systems reveal flux-tube or stringlike structures [24,25]. Such flux-tube-like structures lead to a multibody confinement interaction which is proportional to the minimum of the total length of flux tubes [24,25]. Based on the traditional quark models and LQCD picture, a color flux-tube model has been developed, in which the confinement is a multibody interaction instead of the sum of two-body one in the traditional model. In order to simplify the numerical calculation the linear multibody confinement is replaced by a harmonic one, i.e., lengths of flux tubes are replaced by the square of lengths [26,27]. This approximation is justified because of the following two reasons: one is that the spatial variations in separation of the quarks (lengths of the flux tube) in different hadrons do not differ significantly, so the difference between the two functional forms is small and can be absorbed in the adjustable parameter, the stiffness of a flux tube. The other is that we are using a nonrelativistic equation in the study. As was shown long time ago [28], an interaction energy that varies linearly with separation between fermions in a relativistic first order differential equation has a wide region in which a harmonic approximation is valid for the second order (Feynman-Gell-Mann) reduction of the equation. The comparative studies also indicated that the difference between the quadratic confinement potential and the linear one is very small [26,27]. The color flux-tube model can avoid the color van der Waals forces between color-singlet hadrons and the anticonfinement in color symmetrical quark or antiquark pair in the traditional models.

The color flux-tube structure of an ordinary hadron is unique and trivial, the multibody quadratic confinement potential is equivalent to the two-body color dependent interactions [17]. In this sense, the color flux-tube model is reduced to the traditional quark model for ordinary hadrons. For multiquark hadrons the situation is changed

because the systems have various color flux-tube structures in the intermediate- and short-distance ranges and the corresponding multibody confinement potential is no longer equivalent to the two-body ones. The color flux-tube structures of multiquark states can provide more low-energy QCD information than ordinary hadrons, such as a quark pair with symmetric color representations. The previous research on the light tetraquark spectrum indicated that a tetraquark system has at least four color flux-tube structures [15]: meson-meson molecule $[q\bar{q}]_1[q\bar{q}]_1$, hidden color octet-antioctet $[[q\bar{q}]_8[q\bar{q}]_8]_1$, diquark-antidiquark $[[qq]_3[\bar{q}\,\bar{q}]_{\bar{3}}]_1$ or $[[qq]_6[\bar{q}\,\bar{q}]_{\bar{6}}]_1$, and ringlike $[qq\bar{q}\,\bar{q}]_1$ (called QCD cyclobutadiene in Ref. [15]). The states with these flux-tube structures are similar to the molecules having the same atomic content but different molecular bonds and can be called QCD isomers. In general, a tetraquark state should be a mixture of all of these QCD isomer states [15]. In order to avoid too complicated numerical calculations, the diquark-antidiquark structure is considered in the present work. The diquark-antidiquark structure has been used in many model calculations [29] (but no sound theoretical reason to neglect the other structures).

Within the color flux-tube model, the confinement potential of the diquark-antidiquark structure can be expressed as

$$V^{\rm CON}(4) = K((\mathbf{r}_1-\mathbf{y}_{12})^2+(\mathbf{r}_2-\mathbf{y}_{12})^2+(\mathbf{r}_3-\mathbf{y}_{34})^2 + (\mathbf{r}_4-\mathbf{y}_{34})^2+\kappa_d(\mathbf{y}_{12}-\mathbf{y}_{34})^2), \quad (2)$$

where $\mathbf{r}_1$ and $\mathbf{r}_2$ represent the two quarks' positions, $\mathbf{r}_3$ and $\mathbf{r}_4$ represent the two antiquarks' positions, and the variational parameters $\mathbf{y}_{12}$ and $\mathbf{y}_{34}$ represent the two Y-shaped junction positions where three flux tubes meet. The parameter K is the stiffness of a three-dimensional flux-tube, $\kappa_d K$ is other compound color flux-tube stiffness. The relative stiffness parameter κ_d [30] of the compound flux-tube is

$$\kappa_d = \frac{C_d}{C_3}, \quad (3)$$

where C_d is the eigenvalue of the Casimir operator associated with the $SU(3)$ color representation d at either end of the color flux-tube, namely, $C_3=\frac{4}{3}$, $C_6=\frac{10}{3}$, and $C_8=3$.

For given quark (antiquark) positions $\mathbf{r}_i$, the junctions $\mathbf{y}_{12}$ and $\mathbf{y}_{34}$ can be fixed by minimizing the confinement potential. It is understood here that the gluon field readjusts immediately to its minimal configuration. By introducing the following set of canonical coordinates $\mathbf{R}_i$,

$$\mathbf{R}_1=\frac{1}{\sqrt{2}}(\mathbf{r}_1-\mathbf{r}_2), \qquad \mathbf{R}_2=\frac{1}{\sqrt{2}}(\mathbf{r}_3-\mathbf{r}_4),$$
$$\mathbf{R}_3=\frac{1}{\sqrt{4}}(\mathbf{r}_1+\mathbf{r}_2-\mathbf{r}_3-\mathbf{r}_4),$$
$$\mathbf{R}_4=\frac{1}{\sqrt{4}}(\mathbf{r}_1+\mathbf{r}_2+\mathbf{r}_3+\mathbf{r}_4), \quad (4)$$

the minimum $V^{\rm CON}_{\rm min}(4)$ of the confinement potential reduces to the sum of three independent harmonic oscillators,

$$V^{\rm CON}_{\rm min}(4) = K\left(\mathbf{R}_1^2+\mathbf{R}_2^2+\frac{\kappa_d}{1+\kappa_d}\mathbf{R}_3^2\right). \quad (5)$$

Clearly, the confinement $V^{\rm CON}_{\rm min}(4)$ is a four-body interaction and cannot be reduced to the sum of six pairs two-body interactions. For a two-body system, an ordinary meson, the confinement potential can be written as

$$V^{\rm CON}_{\rm min}(2) = Kr^2, \quad (6)$$

where the r is the separation of the quark and antiquark of a meson.

In addition to the color confinement, there are other interactions, one-boson-exchange and one-gluon-exchange potentials between quarks (antiquarks). Here we only write down their forms; the details can be found in many papers, for example Ref. [20],

$$V^B_{ij} = V^\pi_{ij}\sum_{k=1}^{3}\mathbf{F}_i^k\mathbf{F}_j^k + V^K_{ij}\sum_{k=4}^{7}\mathbf{F}_i^k\mathbf{F}_j^k + V^\eta_{ij}(\mathbf{F}_i^8\mathbf{F}_j^8\cos\theta_P - \mathbf{F}_i^0\mathbf{F}_j^0\sin\theta_P), \quad (7)$$

$$V^\chi_{ij} = \frac{g_{ch}^2}{4\pi}\frac{m_\chi^3}{12m_im_j}\frac{\Lambda_\chi^2}{\Lambda_\chi^2-m_\chi^2}\boldsymbol{\sigma}_i\cdot\boldsymbol{\sigma}_j \times\left(Y(m_\chi r_{ij})-\frac{\Lambda_\chi^3}{m_\chi^3}Y(\Lambda_\chi r_{ij})\right), \qquad \chi=\pi,K,\eta$$
$$V^\sigma_{ij} = -\frac{g_{ch}^2}{4\pi}\frac{\Lambda_\sigma^2}{\Lambda_\sigma^2-m_\sigma^2}m_\sigma\left(Y(m_\sigma r_{ij})-\frac{\Lambda_\sigma}{m_\sigma}Y(\Lambda_\sigma r_{ij})\right),$$
$$V^G_{ij} = \frac{1}{4}\alpha_s\boldsymbol{\lambda}_i^c\cdot\boldsymbol{\lambda}_j^c\left(\frac{1}{r_{ij}}-\frac{2\pi\delta(\mathbf{r}_{ij})\boldsymbol{\sigma}_i\cdot\boldsymbol{\sigma}_j}{3m_im_j}\right), \quad (8)$$

where $Y(x)$ is standard Yukawa potential, $Y(x)=e^{-x}/x$. The symbols $\mathbf{F}$, $\boldsymbol{\lambda}$ and $\boldsymbol{\sigma}$ are the flavor $SU(3)$, color SU(3) Gell-Mann and spin $SU(2)$ Pauli matrices, respectively. θ_P is the mixing angle between η_1 and η_8 to give the physical η meson. m_i is the mass of the ith quark. $g_{ch}^2/4\pi$ is the chiral coupling constant. α_s is the running strong coupling constant and takes the following form [31],

$$\alpha_s(\mu_{ij}) = \frac{\alpha_0}{\ln\left((\mu_{ij}^2+\mu_0^2)/\Lambda_0^2\right)}, \tag{9}$$

where μ_{ij} is the reduced mass of two interacting quarks q_i and q_j. Λ_0, α_0 and μ_0 are model parameters. The function $\delta(\mathbf{r}_{ij})$ in V_{ij}^G should be regularized [32],

$$\delta(\mathbf{r}_{ij}) = \frac{1}{4\pi r_{ij} r_0^2(\mu_{ij})} e^{-r_{ij}/r_0(\mu_{ij})}, \tag{10}$$

with $r_0(\mu_{ij}) = \hat{r}_0/\mu_{ij}$, where $\hat{r}_0$ is a model parameter.

To sum up, the total Hamiltonian H_f in the color flux-tube model can be expressed as follows:

$$H_f = \sum_{i=1}^{f}\left(m_i + \frac{\mathbf{p}_i^2}{2m_i}\right) - T_C + \sum_{i>j}^{f} V_{ij} + V_{\min}^C(f),$$
$$V_{ij} = V_{ij}^B + V_{ij}^\sigma + V_{ij}^G. \tag{11}$$

In the above expression of H_f, $f = 2$ or 4, T_c is the center-of-mass kinetic energy, and $\mathbf{p}_i$ is the momentum of the ith quark. The tensor and spin-orbit forces between quarks are omitted in the present calculation because, for the lowest energy states which we are interested in here, their contributions are small or zero. The present study involves up, down, strange, charm and bottom quarks, and the details of the interactions are listed in the following,

$$V_{ij} = \begin{cases} V_{ij}^G + V_{ij}^\pi + V_{ij}^\eta + V_{ij}^\sigma & q_iq_j = nn \\ V_{ij}^G + V_{ij}^K + V_{ij}^\eta + V_{ij}^\sigma & q_iq_j = ns \\ V_{ij}^G + V_{ij}^\eta + V_{ij}^\sigma & q_iq_j = ss \\ V_{ij}^G & q_iq_j = Qn \\ V_{ij}^G & q_iq_j = Qs \\ V_{ij}^G & q_iq_j = QQ \end{cases}, \tag{12}$$

where n stands for the nonstrange light quarks, u and d, and Q represents a charm or bottom quark. As far as ordinary mesons are concerned, the Hamiltonian H_2 in the color flux-tube model is almost the same as that in the chiral quark model [31]. However, if the color flux-tube model is applied to multiquark states, the multibody confinement potential instead of a color dependent two-body one is used so that it can overcome the shortcomings of traditional quark models. In fact, the color flux-tube model based on traditional quark models and LQCD picture merely modifies the two-body confinement potential to describe multiquark states with multibody interactions.

III. WAVE FUNCTIONS OF CHARGED TETRAQUARK STATES

In the diquark-antidiquark configuration, the wave function of a tetraquark state $[Qq][\bar{Q}'\bar{q}']$ can be written as a sum of the following direct products of color, isospin, spin and spatial terms [33,34],

$$\Phi_{IM_IJM_J}^{[Qq][\bar{Q}'\bar{q}']} = \sum_\alpha \xi_\alpha [[[\phi_{l_am_a}^G(\mathbf{r})\chi_{s_a}]_{j_a}^{[Qq]} \times [\psi_{l_bm_b}^G(\mathbf{R})\chi_{s_b}]_{j_b}^{[\bar{Q}'\bar{q}']}]_{J_{ab}}^{[Qq][\bar{Q}'\bar{q}']} F_{LM}(\mathbf{X})]_{JM_J}^{[Qq][\bar{Q}'\bar{q}']} \times [\eta_{I_a}^{[Qq]}\eta_{I_b}^{[\bar{Q}'\bar{q}']}]_{IM_I}^{[Qq][\bar{Q}'\bar{q}']} [\chi_{c_a}^{[Qq]}\chi_{c_b}^{[\bar{Q}'\bar{q}']}]_{CW_C}^{[Qq][\bar{Q}'\bar{q}']}. \tag{13}$$

The codes of the quarks Q and q, and the antiquarks $\bar{Q}'$ and $\bar{q}'$ are assumed to be 1 and 2, and 3 and 4, respectively. In the frame of center of mass, three relative motion coordinates, $\mathbf{r}$, $\mathbf{R}$, and $\mathbf{X}$, can be expressed as

$$\mathbf{r} = \mathbf{r}_1 - \mathbf{r}_2, \qquad \mathbf{R} = \mathbf{r}_3 - \mathbf{r}_4,$$
$$\mathbf{X} = \frac{m_1\mathbf{r}_1 + m_2\mathbf{r}_2}{m_1+m_2} - \frac{m_3\mathbf{r}_3 + m_4\mathbf{r}_4}{m_3+m_4}. \tag{14}$$

The total kinetic energy T of the state $[Qq][\bar{Q}'\bar{q}']$ in the frame of center of mass can therefore be written as

$$T = \sum_{i=1}^{4}\frac{\mathbf{p}_i^2}{2m_i} - T_c = \frac{\mathbf{p}_\mathbf{r}^2}{2\mu_\mathbf{r}} + \frac{\mathbf{p}_\mathbf{R}^2}{2\mu_\mathbf{R}} + \frac{\mathbf{p}_\mathbf{X}^2}{2\mu_\mathbf{X}}, \tag{15}$$

where $\mu_\mathbf{r}$, $\mu_\mathbf{R}$, and $\mu_\mathbf{X}$ are the corresponding reduced masses [35], l_a, l_b, and L are the orbital angular momenta associated with the relative motions $\mathbf{r}$, $\mathbf{R}$, and $\mathbf{X}$, respectively, and J is the total angular momentum. I_a, I_b are the isospins of the clusters $[Qq]$ and $[\bar{Q}'\bar{q}']$, respectively, and I is the total isospin. α represents all possible intermediate quantum numbers, $\alpha = \{l_k, s_k, j_k, J_{ab}, L, I_k\}, k = a, b$. χ_{s_k}, η_{I_k}, and χ_{c_k} stand for spin, flavor, and color wave functions of the diquark $[Qq]$ or the antidiquark $[\bar{Q}'\bar{q}']$, respectively. [ ]'s denote Clebsh-Gordan coefficient coupling. The overall color singlet can be constructed in two possible ways: $\chi_c^1 = \bar{3}_{12} \otimes 3_{34}$ and $\chi_c^2 = 6_{12} \otimes \bar{6}_{34}$. The so-called "good" diquark ($c_a = \bar{3}$ and $j_a^P = 0^+$, $c_b = 3$ and $j_b^P = 0^+$), the "bad" diquark ($c_a = \bar{3}$ and $j_a^P = 1^+$, $c_b = 3$ and $j_b^P = 1^+$), and the "worse" diquark (others) are all included. The Jaffe's terminology of the diquark is used here. The first two and the last one were also formerly called "true" and "mock" diquarks, respectively [29,36]. The coefficient ξ_α is determined by diagonalizing the Hamiltonian.

The diquark $[Qq]$ (antidiquark $[\bar{Q}'\bar{q}']$) can be considered as a new compound object $\bar{\mathcal{Q}}$ ($\mathcal{Q}'$) with no internal orbital excitations, and the excitations are assumed to occur only between $\mathcal{Q}'$ and $\bar{\mathcal{Q}}$ in the present numerical calculations, such a tetraquark state has lower energy than the states with additional internal orbital excitation. The orbital angular momenta l_a and l_b are therefore assumed to be zero in the present work. Under these assumptions, $s_a = j_a$, $s_b = j_b$, $S = s_a + s_b = j_a + j_b = J_{ab}$, and $J = L + S$, where S can

take the value 0, 1, and 2. The parity of a tetraquark with these diquark-antidiquark structures is simply related to L as $P = (-1)^L$.

To obtain a reliable numerical solution of a few-body problem, a high-precision method is indispensable. The GEM [37], which has been proven to be rather powerful in solving few-body problems, is used to study four-body systems in the flux-tube model. In the GEM, three relative motion wave functions can be expanded as

$$\phi^G_{l_a m_a}(\mathbf{r}) = \sum_{n_a=1}^{n_{a\times\max}} c_{n_a} N_{n_a l_a} r^{l_a} e^{-\nu_{n_a} r^2} Y_{l_a m_a}(\hat{\mathbf{r}}),$$
$$\psi^G_{l_b m_b}(\mathbf{R}) = \sum_{n_b=1}^{n_{b\times\max}} c_{n_b} N_{n_b l_b} R^{l_b} e^{-\nu_{n_b} R^2} Y_{l_b m_b}(\hat{\mathbf{R}}),$$
$$F^G_{LM}(\mathbf{X}) = \sum_{n_c=1}^{n_{c\times\max}} c_{n_c} N_{n_c L} X^L e^{-\nu_{n_c} X^2} Y_{LM}(\hat{\mathbf{X}}), \quad (16)$$

where $N_{n_a l_a}$, $N_{n_b l_b}$, and $N_{n_c L}$ are normalization constants. Gaussian size parameters are taken as the following geometric progression numbers:

$$\nu_n = \frac{1}{r_n^2}, \qquad r_n = r_1 x^{n-1}, \qquad x = \left(\frac{r_{n_{\max}}}{r_1}\right)^{\frac{1}{n_{\max}-1}}. \quad (17)$$

The geometric progression leads to that ν_n is denser at intermediate and short ranges than at long ranges, so that it is suited to describe the dynamics mediated by intermediate- and short-range interactions.

IV. NUMERICAL RESULTS AND DISCUSSIONS

A lot of research has been devoted to studying the meson spectrum in different quark models [31,38,39]. The heavy mesons, such as charmonium, are properly described by nonrelativistic potential models incorporating both the Coulomb and confinement forces [38]. The mesons from the π to Υ can be described in a relativized quark model with a universal one-gluon exchange plus a linear confining potential motivated by QCD [39]. In the same way, the spectrum from the light-pseudoscalar and vector mesons to bottomonium are also investigated in a nonrelativistic quark model with one gluon exchange potential, a screened confinement, and one boson exchange [31]. The meson spectrum is the starting point of the studies of tetraquark states in our color-flux tube model, and all the model parameters are fixed by meson spectrum. The model parameters are determined as follows. The mass parameters m_π, m_K, and m_η in the interaction V^B_{ij} take their experimental values, namely, $m_\pi = 0.7$ fm^{-1}, $m_K = 2.51$ fm^{-1}, $m_\eta = 2.77$ fm^{-1}. The mass parameter m_σ in the interaction V^σ_{ij} is determined through the PCAC relation $m_\sigma^2 \sim m_\pi^2 + 4m_{u,d}^2$ [40], $m_{u,d} = 280$ MeV, $m_\sigma = 2.92$ fm^{-1}. The cutoff parameters take the values, $\Lambda_\pi = \Lambda_\sigma = 4.20$ fm^{-1} and $\Lambda_K = \Lambda_\eta = 5.20$ fm^{-1} fixed in [31,41], where the mixing angle $\theta_P = -\pi/12$ [31]. The chiral coupling constant g_{ch} is determined from the πNN coupling constant through

$$\frac{g_{ch}^2}{4\pi} = \left(\frac{3}{5}\right)^2 \frac{g_{\pi NN}^2}{4\pi} \frac{m_{u,d}^2}{m_N^2} = 0.43. \quad (18)$$

The other adjustable parameters and their errors are fixed by fitting the masses of mesons using Minuit program. The mass spectrum of the ground states of mesons from π to Υ can be obtained by solving the two-body Schrödinger equation

$$(H_2 - E_{IJ})\Phi^{q\bar{q}}_{IJ} = 0 \quad (19)$$

with Rayleigh-Ritz variational principle in the color flux-tube model. The converged numerical results can be reached by setting $r_1 = 0.1$ fm, $r_{n_{\max}} = 2.0$ fm and $n_{\max} = 7$. The benchmark identifying whether the variational results are convergent or not is that the results are stable against the varying of the number of Gaussians $n_{\max}$. Table I shows that the stability of our results against the number of Gaussians, where the meson $D^\pm$ and the charged tetraquark states Z_c which will be discussed in the following part of this section are taken as examples. The adjustable parameters and their errors are shown in Table II and the fitted meson spectra and their errors are given in Table III. The larger errors of π and K mesons come from the stronger interactions in π and K mesons. From Table III, one can find that the heavy mesons, $D^\pm$, D^*, $D_s^\pm$, D_s^*, B^0, B^*, B_s^0 and B_s^*, involved in the tetraquark calculations are preferentially taken into account. For comparison, the results of the other two models are also listed in the Table III. Generally speaking, other two models can

TABLE I. The stabilities of calculated results against the number of Gaussians, units in MeV.

$n_{\max}$	2	3	4	5	6	7	8
$D^\pm$	6805.8	3142.7	2128.0	1882.2	1867.2	1867.1	1867.1
Z_c	4588.9	4091.1	4006.2	4000.6	4000.5	4000.5	4000.5

TABLE II. The adjustable parameters and their errors in the color flux-tube model. (units: m_s, m_c, m_b, μ_0, Λ, MeV; K, MeV $\cdot$ fm^{-2}; r_0, MeV $\cdot$ fm; α_0, dimensionless)

Parameters	Values	Errors	Parameters	Values	Errors
m_s	511.78	0.228	α_0	4.554	0.018
m_c	1601.7	0.441	Λ_0	9.173	0.175
m_b	4936.2	0.451	μ_0	0.0004	0.540
K	217.50	0.230	r_0	35.06	0.156

TABLE III. The ground state meson spectra and their errors, units in MeV.

Mesons	IJ^P	E_{IJ}	ΔE_{IJ}	Ref. [38]	Ref. [31]	PDG
π	10^-	142	26	150	139	139
K	$\frac{1}{2}0^-$	492	20	470	496	496
ρ	11^-	826	4	770	772	775
ω	01^-	780	4	780	690	783
K^*	$\frac{1}{2}1^-$	974	4	900	910	892
ϕ	01^-	1112	4	1020	1020	1020
$D^{\pm}$	$\frac{1}{2}0^-$	1867	8	1880	1883	1869
D^*	$\frac{1}{2}1^-$	2002	4	2040	2010	2007
$D_s^{\pm}$	00^-	1972	9	1980	1981	1968
D_s^*	01^-	2140	4	2130	2112	2112
η_c	00^-	2912	5	2970	2990	2980
J/Ψ	01^-	3102	4	3100	3097	3097
B^0	$\frac{1}{2}0^-$	5259	5	5310	5281	5280
B^*	$\frac{1}{2}1^-$	5301	4	5370	5321	5325
B_s^0	00^-	5377	5	5390	5355	5366
B_s^*	01^-	5430	4	5450	5400	5416
B_c	00^-	6261	7	6270	6277	6277
B_c^*	01^-	6357	4	6340	...	...
η_b	00^-	9441	8	9400	9454	9391
$\Upsilon(1S)$	01^-	9546	5	9460	9505	9460

describe the meson spectra a little better than our model. However, the number of the free parameters in our model is two less than those in the model of Ref [31].

The color flux-tube model with the parameters listed in Table II is used to investigate the charge tetraquark states $[Qq][\bar{Q}'\bar{q}']$. It should be emphasized that no any new parameters or assumptions are introduced in the course of the calculation. We focus our attentions on the lowest charged states $[Qq][\bar{Q}'\bar{q}']$, and therefore the orbital angular momentum between two clusters is set to be 0, then parity $P = +$, isospin $I = \frac{1}{2}$ or 1, and the total angular momentum $J = 0$, 1 and 2. In order to observe the underlying phenomenological features, a systematical calculations on the charged tetraquark states $[Qq][\bar{Q}'\bar{q}']$ are carried out. The energies of the tetraquark states $[Qq][\bar{Q}'\bar{q}']$ can be obtained by solving the four-body Schrödinger equation,

$$(H_4 - E_{IJ})\Phi_{IM_IJM_J}^{[Qq][\bar{Q}'\bar{q}']} = 0. \tag{20}$$

The converged numerical results can be obtained by setting $n_{a\times\max} = 6$, $n_{b\times\max} = 6$ and $n_{c\times\max} = 6$ (see Table I). The minimum and maximum ranges of the bases are 0.3 fm and 2.0 fm for the coordinates $\mathbf{r}$, $\mathbf{R}$, and $\mathbf{X}$, respectively.

The lowest energies E_{IJ} and their errors ΔE_{IJ} are given in Table IV, where the errors are around 10 MeV. The stability of these states can be identified by the binding energies corresponding to the meson-meson thresholds $T_{M_1M_2} = M_1(Q\bar{q}') + M_2(\bar{Q}'q)$ and $T_{M_1'M_2'} = M_1(Q\bar{Q}') + M_2(q\bar{q}')$, where the binding energies are defined as $E_B = E_{IJ} - T_{M_1M_2}$ and $E_B' = E_{IJ} - T_{M_1'M_2'}$. If $E_B, E_B' < 0$, then the states $[Qq][\bar{Q}'\bar{q}']$ are bound states and cannot decay into two corresponding color singlet mesons $Q\bar{q}'$ and $\bar{Q}'q$, $Q\bar{Q}'$ and $q\bar{q}'$ under the strong interaction. While if $E_B > 0$ and (or) $E_B' > 0$, the states $[Qq][\bar{Q}'\bar{q}']$ may be resonances and can decay into two corresponding color singlet mesons through the rupture and rearrangement of the color flux tubes. The errors ΔE_B and $\Delta E_B{}'$ of the binding energies E_B and $E_B{}'$, respectively, are calculated and listed in Table IV. One can find that the errors ΔE_B are small and less than 3 MeV because of the error cancellation in the expressions of the binding energies E_B. However, the errors $\Delta E_B{}'$ of the states with $J = 0$ and 1 are around 10 MeV because of the big errors of π and K mesons in the errors $\Delta E_B{}'$.

It can be seen from Table IV that the energies E_{IJ} of all of these states are higher than the corresponding threshold $T_{M_1'M_2'}$, due to the large binding energies of the light mesons, π, ρ, K, and K^*, which originate from the stronger interactions between two light quarks q and $\bar{q}'$. The binding energies E_B' of the low-spin ($S = 0$ or 1) tetraquark states $[Qq][\bar{Q}'\bar{q}']$ are several hundreds of MeV higher, while E_B' of the high-spin ($S = 2$) states are only several tens of MeV higher, than the corresponding threshold $T_{M_1'M_2'}$. The difference is due to the smaller masses of pseudoscalar mesons in the decay products of the low-spin states. So the charged states $[Qq][\bar{Q}'\bar{q}']$ are hard to form bound tetraquark states and can finally decay into two mesons $Q\bar{Q}'$ and $q\bar{q}$, which is in agreement with the conclusions of the work [33,42]. On the contrary, the states $[QQ][\bar{q}\,\bar{q}]$ are easier to form stable tetraquark states due to that they can only decay into two $Q\bar{q}$ mesons in the quark model [33,43].

The energies E_{IJ} of the states $[Qq][\bar{Q}'\bar{q}']$ are also compared with the threshold $T_{M_1M_2}$. From Table IV, it can be found that the energies of many states lie below the thresholds $T_{M_1M_2}$, i.e., $E_B < 0$. Let us first pay attention to the charged states $[cu][\bar{c}\,\bar{d}]$. The energies E_{IJ} with $IJ = 11$ and 12 are lower than the thresholds of $D^*\bar{D}$ or $D\bar{D}^*$ and $D^*\bar{D}^*$ by 11 and 3 MeV, respectively. So these two states cannot decay into $D^*\bar{D}$ or $D\bar{D}^*$ and $D^*\bar{D}^*$ through strong interactions. After taking the meson mass differences between the calculated one and the experimental one into account (see Table III), the energies E_{IJ} of the states with $IJ = 11$ and 12 should be about 3865 and 4011 MeV, respectively, which are very close to the results of Ref. [44], where the heavy tetraquark states are considered as the bound states of a heavy-light diquark and antidiquark in the framework of the relativistic quark model. The color flux-tube model energies of the charged states $[cu][\bar{c}\,\bar{d}]$ with $IJ = 11$ and 12 are in good agreement with the masses of the observed $Z_c(3900)$ and $Z_c(4025)/Z_c(4020)$, respectively [4–9]. The dominant component of the charged sates $Z_c(3900)$ and $Z_c(4025)/Z_c(4020)$ might therefore be the hidden color tetraquark states $[cu][\bar{c}\,\bar{d}]$ with $IJ^P = 11^+$ and 12^+, respectively. This identification of the charged Z_c

TABLE IV. The energies E_{IJ}, binding energies E_B and E'_B and their errors ΔE_{IJ}, ΔE_B and $\Delta E'_B$ (unit in MeV) of the charge tetraquark states $[Qu][\bar{Q}'\bar{d}]$ and $[Qu][\bar{Q}'\bar{s}]$ in the S-wave ($L=0$), and the rms $\langle\mathbf{r}^2\rangle^{\frac{1}{2}}$, $\langle\mathbf{R}^2\rangle^{\frac{1}{2}}$ and $\langle\mathbf{X}^2\rangle^{\frac{1}{2}}$ (unit in fm) of the clusters $[Qq]$, $[\bar{Q}'\bar{q}']$ and $[Qq]$-$[\bar{Q}'\bar{q}']$, respectively.

States	$[cu][\bar{c}\,\bar{d}]$			$[bu][\bar{b}\,\bar{d}]$			$[cu][\bar{b}\,\bar{d}]$		
IJ^P	10^+	11^+	12^+	10^+	11^+	12^+	10^+	11^+	12^+
E_{IJ}	3782	3858	4001	10317	10342	10484	7084	7122	7266
ΔE_{IJ}	12	10	7	11	10	8	11	10	8
$T_{M_1M_2}$	$D\bar{D}$	$D\bar{D}^*/D^*\bar{D}$	$D^*\bar{D}^*$	$B\bar{B}$	$B\bar{B}^*/B^*\bar{B}$	$B^*\bar{B}^*$	$D\bar{B}$	$D\bar{B}^*/D^*\bar{B}$	$D^*\bar{B}^*$
E_B	48	−11	−3	−201	−218	−118	−42	−46/−139	−37
ΔE_B	2	1	1	1	1	1	1	1/1	1
$T_{M'_1M'_2}$	$\pi\eta_c$	$\pi J/\Psi/\rho\eta_c$	$\rho J/\Psi$	$\pi\eta_b$	$\pi\Upsilon(1S)/\rho\eta_b$	$\rho\Upsilon(1S)$	$\pi\bar{B}_c$	$\pi\bar{B}^*_c/\rho\bar{B}_c$	$\rho\bar{B}^*_c$
$E_B{}'$	728	614/120	73	734	654/75	112	681	623/35	83
$\Delta E'_B$	12	10/2	1	12	11/1	1	11	10/1	1
$\langle\mathbf{r}^2\rangle^{\frac{1}{2}}$	0.85	0.90	1.03	0.85	0.86	1.01	0.86	0.89	1.01
$\langle\mathbf{R}^2\rangle^{\frac{1}{2}}$	0.85	0.90	1.03	0.85	0.86	1.01	0.84	0.86	1.01
$\langle\mathbf{X}^2\rangle^{\frac{1}{2}}$	0.42	0.48	0.57	0.27	0.28	0.29	0.36	0.39	0.45

States	$[cu][\bar{c}\,\bar{s}]$			$[bu][\bar{b}\,\bar{s}]$			$[bu][\bar{c}\,\bar{s}]$			$[cu][\bar{b}\,\bar{s}]$		
IJ^P	$\frac{1}{2}0^+$	$\frac{1}{2}1^+$	$\frac{1}{2}2^+$	$\frac{1}{2}0^+$	$\frac{1}{2}1^+$	$\frac{1}{2}2^+$	$\frac{1}{2}0^+$	$\frac{1}{2}1^+$	$\frac{1}{2}2^+$	$\frac{1}{2}0^+$	$\frac{1}{2}1^+$	$\frac{1}{2}2^+$
E_{IJ}	3998	4065	4162	10529	10552	10645	7302	7334	7432	7293	7328	7423
ΔE_{IJ}	11	9	7	10	10	8	10	9	7	10	9	7
$T_{M_1M_2}$	$D_s\bar{D}$	$D_s\bar{D}^*/D^*_s\bar{D}$	$D^*_s\bar{D}^*$	$B_s\bar{B}$	$B_s\bar{B}^*/B^*_s\bar{B}$	$B^*_s\bar{B}^*$	$\bar{D}B_s$	$\bar{D}B^*_s/\bar{D}^*B_s$	$\bar{D}^*B^*_s$	$D_s\bar{B}$	$D_s\bar{B}^*/D^*_s\bar{B}$	$D^*_s\bar{B}^*$
E_B	159	91/58	20	−107	−126/−137	−86	58	37/−45	−1	62	55/−71	−18
ΔE_B	3	2/1	1	1	1/1	1	2	1/1	1	2	2/1	1
$T_{M'_1M'_2}$	$K\eta_c$	$KJ/\Psi/K^*\eta_c$	K^*J/Ψ	$K\eta_b$	$K\Upsilon(1S)/K^*\eta_b$	$K^*\Upsilon(1S)$	KB_c	KB^*_c/K^*B_c	$K^*B^*_c$	$K\bar{B}_c$	$K\bar{B}^*_c/K^*\bar{B}_c$	$K^*\bar{B}^*_c$
$E_B{}'$	594	471/179	86	596	514/137	125	549	485/99	101	540	479/93	92
$\Delta E'_B$	10	7/3	1	9	8/2	1	8	8/1	1	8	7/1	1
$\langle\mathbf{r}^2\rangle^{\frac{1}{2}}$	0.85	0.90	1.01	0.86	0.87	0.99	0.75	0.76	0.87	0.87	0.75	1.00
$\langle\mathbf{R}^2\rangle^{\frac{1}{2}}$	0.74	0.80	0.88	0.74	0.75	0.84	0.84	0.86	0.99	0.73	0.90	0.85
$\langle\mathbf{X}^2\rangle^{\frac{1}{2}}$	0.43	0.59	0.56	0.27	0.28	0.29	0.37	0.40	0.45	0.37	0.40	0.44

states as tetraquark states is in agreement with previous ones [11]. As for the state $[cu][\bar{c}\,\bar{d}]$ with $IJ^P=10^+$, the energy is about 3786 MeV and very close to the results of hadro-quarkonium model [13], where the state $[cu][\bar{c}\,\bar{d}]$ with $I^GJ^P=1^-0^+$ was called W_c.

Next, let us turn to the charged tetraquark states of hidden charm and open strangeness, namely the state $[cu][\bar{c}\,\bar{s}]$ or $[cs][\bar{c}\,\bar{u}]$. Table IV shows that the energies of the states with $IJ=\frac{1}{2}0$ and $\frac{1}{2}1$ are much higher than the thresholds $\bar{D}_sD$ and $\bar{D}_sD^*$, respectively. While the energies of the states $[cu][\bar{c}\,\bar{s}]$ with $IJ=\frac{1}{2}1$ and $\frac{1}{2}2$ are close to the thresholds $\bar{D}^*_sD$ and $\bar{D}^*_sD^*$, respectively. Taking into account the meson mass differences between the calculated and the experimental ones again, the predicted $[cu][\bar{c}\,\bar{s}]$ with $IJ=\frac{1}{2}1$ and $\frac{1}{2}2$ energies are about 4039 and 4139 MeV, respectively. The masses of these states obtained by the initial single chiral particle emission model are also near the thresholds of $\bar{D}^*_sD/\bar{D}_sD^*$ and $\bar{D}^*_sD^*/D^*_s\bar{D}^*$ [45]. So we suggest to study these charged charmoniumlike states with hidden-charm and open-strangeness further. The hidden-beauty partners of the charged hidden charm states have rather strong binding in the color flux-tube model, see Table IV. Their masses in the model are much lower than experimental ones of the charged states $Z_b(10610)$ and $Z_b(10650)$ [3]. Therefore, the main components of these two states are hard to be described as charged tetraquark states $[bu][\bar{b}\,\bar{d}]$ in the color flux-tube model. However the chiral quark model calculation showed that they are [46]. For the other open-charm and open-beauty charged states $[cu][\bar{b}\,\bar{d}]$, $[bu][\bar{c}\,\bar{s}]$ and $[cu][\bar{b}\,\bar{s}]$, the energies are very close to the corresponding thresholds, which we also suggest to search in the future.

In addition, one can, from Table IV, find that the bigger the mass ratios M_Q/m_q and $M_{\bar{Q}'}/m_{\bar{q}'}$ in the different charged states $[Qq][\bar{Q}'\bar{q}']$ but with the same IJ, the bigger the corresponding binding energies E_B. Taking the states with $IJ=11$ as an example, we have $E_B=-11$ MeV for $[cu][\bar{c}\,\bar{d}]$, $-46/-139$ MeV for $[cu][\bar{b}\,\bar{d}]$ and -218 or $[bu][\bar{b}\,\bar{d}]$. In order to clarify the origin of this tendency, the contributions of various parts of the Hamiltonian to the binding energies E_B of the charged states with $IJ=11$ and 12 are calculated and given in Table V. One can find that the contributions to the binding energy, $\Delta V^{\rm CON}$, $\Delta V^{\rm CM}$ (color-magnetic), ΔV^{σ}, ΔV^{B}, and ΔT, do not have big variation with the mass ratios M_Q/m_q and $M_{\bar{Q}'}/m_{\bar{q}'}$ in the group $[cu][\bar{c}\,\bar{d}]$-$[cu][\bar{b}\,\bar{d}]$-$[bu][\bar{b}\,\bar{d}]$ for $IJ=12$. However, the

TABLE V. The contributions of the various parts of the Hamiltonian in the color flux-tube model to the binding energies E_B of the states with $IJ = 11$ and 12, unit in MeV.

IJ	11			12		
States	$[cu][\bar{c}\,\bar{d}]$	$[cu][\bar{b}\,\bar{d}]$	$[bu][\bar{b}\,\bar{d}]$	$[cu][\bar{c}\,\bar{d}]$	$[cu][\bar{b}\,\bar{d}]$	$[bu][\bar{b}\,\bar{d}]$
$T_{M_1M_2}$	$D\bar{D}^*$	$D\bar{B}^*/D^*\bar{B}$	$B\bar{B}^*$	$D^*\bar{D}^*$	$D^*\bar{B}^*$	$B^*\bar{B}^*$
$\Delta V^{\rm CON}$	−45	−48/−78	−76	−26	−29	−27
ΔV^{CM}	24	26/−108	−96	−8	1	11
$\Delta V^{\rm COU}$	121	77/−4	−85	96	54	−47
ΔV^{B}	−14	−15/−15	−15	3	3	3
ΔV^{σ}	−14	−15/−15	−15	−10	−10	−9
ΔT	−83	−71/81	69	−58	−56	−49
E_B	−11	−46/−139	−218	−3	−37	−118

contribution from the color Coulomb interaction $\Delta V^{\rm COU}$ has a big variation with the mass ratios. For the group $[cu][\bar{c}\,\bar{d}]$-$[cu][\bar{b}\,\bar{d}]$-$[bu][\bar{b}\,\bar{d}]$ with $IJ = 11$, although ΔT is proportional to the mass ratios, the color Coulomb interaction is still the main origin of this tendency [36,47]. The calculated binding energies of charged tetraquark states $[bu][\bar{b}\,\bar{d}]$ might be over estimated in comparison to the charged states $Z_b(10610)$ and $Z_b(10650)$ in the color flux-tube model.

In order to obtain the spatial structure picture of the charged states, the rms $\langle \mathbf{r}^2\rangle^{\frac{1}{2}}$, $\langle \mathbf{R}^2\rangle^{\frac{1}{2}}$ and $\langle \mathbf{X}^2\rangle^{\frac{1}{2}}$, which stand for the sizes of the diquark $[Qq]$, the antidiquark $[\bar{Q}'\bar{q}']$ and the distance between the two clusters, respectively, are calculated and also shown in Table VI. One can find that the $\langle \mathbf{X}^2\rangle^{\frac{1}{2}}$ is inversely proportional to the masses of the diquark $[Qq]$ and antidiquark $[\bar{Q}'\bar{q}']$ and much smaller than the $\langle \mathbf{r}^2\rangle^{\frac{1}{2}}$ and $\langle \mathbf{R}^2\rangle^{\frac{1}{2}}$. So one expects the charged states $[Qq][\bar{Q}'\bar{q}']$ are compact tetraquark states because the diquark $[Qq]$ and the antidiquark $[\bar{Q}'\bar{q}']$ have a large overlap. To show the spatial structure of these tetraquark states more clear, the average distances $\langle \mathbf{r}_{ij}^2\rangle^{\frac{1}{2}}$ between the ith particle and the jth particle in the states $[cu][\bar{c}\,\bar{d}]$ with $IJ = 10$, 11, and 12 are calculated and listed in Table VI, in which the order numbers 1, 2, 3, and 4, respectively, stand for the quarks (antiquarks) c, u, $\bar{c}$ and $\bar{d}$. From Table VI one can find that $\langle \mathbf{r}_{12}^2\rangle^{\frac{1}{2}} = \langle \mathbf{r}_{34}^2\rangle^{\frac{1}{2}} \approx \langle \mathbf{r}_{14}^2\rangle^{\frac{1}{2}} = \langle \mathbf{r}_{23}^2\rangle^{\frac{1}{2}}$ in the same state, thus $\mathbf{r}_{13}$ is approximately perpendicular to $\mathbf{r}_{24}$. The relation $(\langle \mathbf{r}_{12}^2\rangle - \frac{\langle \mathbf{r}_{13}^2\rangle}{4})^{\frac{1}{2}}$ approximatively represents the distance from the u or $\bar{d}$ to the middle point of the $c\bar{c}$. The expression $2(\langle \mathbf{r}_{12}^2\rangle - \frac{\langle \mathbf{r}_{13}^2\rangle}{4})^{\frac{1}{2}} > \langle \mathbf{r}_{24}^2\rangle^{\frac{1}{2}}$ indicates the charged states $[cu][\bar{c}\,\bar{d}]$ in the color flux-tube model must not be planar structures but three-dimensional spatial ones, as shown in Fig. 1, the red dot lines represent color flux tubes which connect four particles to form compact tetraquark states. The situations of other charged states are similar to the states $[cu][\bar{c}\,\bar{d}]$ and also have three-dimensional spatial structures. Such a spatial tetrahedral structure comes from the dynamics of the systems: the color flux tubes shrink the distance between any two connected particles to as short a distance as possible to minimize the confinement potential energy, while the kinetic motion expands the distance between any two quarks to as long a distance as possible to minimize the kinetic energy: the tetrahedral structures meet these requirements better than a planar one does. The four-body confinement potential in the color flux-tube model plays a crucial role in the formation of the three-dimensional compact tetraquark states $[Qq][\bar{Q}'\bar{q}']$. Lattice QCD calculations on tetraquark states also show that a tetrahedral structure is favored because a tetrahedral structure is more stable than a planar one [25]. The multiquark states will be similar to the stereo-chemistry. The color flux-tube model expects a color-stereo chemistry with color isomer.

Due to higher energies of the tetraquark states, they should eventually decay into several color singlet mesons. In the course of the decay, the color flux-tube structure breaks down first which leads to the collapses of the tetrahedral structure, and then through the recombination of the color flux tubes the particles of decay products formed. The decay widths of the charged states $[Qq][\bar{Q}'\bar{q}']$ are determined by the transition probability of the breakdown and recombination of color flux tubes. This decay mechanism is similar to compound nucleus decay and therefore should induce a resonance, which we called it as "color confined, multiquark resonance" state before [48]. It is different from all of those microscopic resonances discussed by S. Weinberg [49]. How to form a multiquark state

TABLE VI. The average distances $\langle \mathbf{r}_{ij}^2\rangle^{\frac{1}{2}}$ between the ith particle and the jth particle in the states $[cu][\bar{c}\,\bar{d}]$ with $IJ = 10$, 11 and 12, unit in fm.

Distances	$\langle \mathbf{r}_{12}^2\rangle^{\frac{1}{2}}$	$\langle \mathbf{r}_{34}^2\rangle^{\frac{1}{2}}$	$\langle \mathbf{r}_{24}^2\rangle^{\frac{1}{2}}$	$\langle \mathbf{r}_{13}^2\rangle^{\frac{1}{2}}$	$\langle \mathbf{r}_{14}^2\rangle^{\frac{1}{2}}$	$\langle \mathbf{r}_{23}^2\rangle^{\frac{1}{2}}$
$IJ = 10$	0.85	0.85	1.11	0.46	0.85	0.85
$IJ = 11$	0.91	0.91	1.20	0.52	0.93	0.93
$IJ = 12$	1.04	1.04	1.38	0.61	1.07	1.07

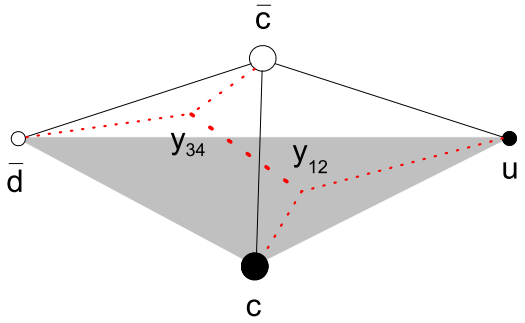

FIG. 1 (color online). The tetrahedral structure of the states $[cu][\bar{c}\,\bar{d}]$.

with flux-tube structure and then decay is an interesting topic for low-energy QCD.

V. SUMMARY

The lowest charged tetraquark states $[Qq][\bar{Q}'\bar{q}']$ $(Q = c, b, q = u, d, s)$ are studied using the variational method GEM in the color flux-tube model with a four-body confinement potential instead of the usual additive two-body confinement. The numerical results indicate that some compact resonance states can be formed, in which the four-body confinement potential is crucial, and they have tetrahedral structures and cannot decay into two color singlet mesons $Q\bar{q}'$ and $\bar{Q}'q$ but into $Q\bar{Q}'$ and $q\bar{q}'$ by means of the breakdown and recombination of the flux tubes. Their decay mechanism is similar to compound nucleus and therefore should induce a so-called "color confined, multiquark resonance" state in the color flux-tube model. The newly observed charged states $Z_c(3900)$ and $Z_c(4025)/Z_c(4020)$ can be accommodated in the color flux-tube model and can be interpreted as the S-wave tetraquark states $[cu][\bar{c}\,\bar{d}]$ with quantum numbers $IJ^P = 11^+$ and 12^+, respectively. The hidden charm and open strangeness charged states are worth the experimental search, while the formation and decay of the exotic quark system with color flux-tube stereo structure is an interesting topic for low-energy QCD. A color stereo chemistry with color isomer world might exist and we might just get into this world.

ACKNOWLEDGMENTS

The authors would like to thank Professor C. P. Shen of Beihang University for his help on the MINUIT program. This research is partly supported by the National Science Foundation of China under Contracts No. 11305274, No. 11175088, No. 11035006, and No. 11205091 and the Chongqing Natural Science Foundation under Project No. cstc2013jcyjA00014.

[1] C. Amsler and N. A. Törnqvist, Phys. Rep. **389**, 61 (2004); E. S. Swanson, Phys. Rep. **429**, 243 (2006); M. Nielsen, F. S. Navarra, and S. H. Lee, Phys. Rep. **497**, 41 (2010); N. Brambilla *et al.*, Eur. Phys. J. C **71**, 1 (2011); R. Faccini, A. Pilloni, and A. D. Polosa, Mod. Phys. Lett. A **27**, 1230025 (2012); G. T. Bodwin, E. Braaten, E. Eichten, S. L. Olsen, T. K. Pedlar, and J. Russ, arXiv:1307.7425.

[2] S. K. Choi *et al.* (BELLE Collaboration), Phys. Rev. Lett. **100**, 142001 (2008); B. Aubert *et al.* (BABAR Collaboration), Phys. Rev. D **79**, 112001 (2009).

[3] A. Bondar *et al.* (Belle Collaboration), Phys. Rev. Lett. **108**, 122001 (2012).

[4] M. Ablikim *et al.* (BES III Collaboration), Phys. Rev. Lett. **110**, 252001 (2013).

[5] Z. Q. Liu *et al.* (Belle Collaboration), Phys. Rev. Lett. **110**, 252002 (2013).

[6] T. Xiao, S. Dobbs, A. Tomaradze, and K. K. Seth, Phys. Lett. B **727**, 366 (2013).

[7] Z. Q. Liu, arXiv:1311.0762.

[8] M. Ablikim *et al.* (BES III Collaboration), Phys. Rev. Lett. **112**, 132001 (2014).

[9] M. Ablikim *et al.* (BES III Collaboration), Phys. Rev. Lett. **111**, 242001 (2013).

[10] Q. Wang, C. Hanhart, and Q. Zhao, Phys. Rev. Lett. **111**, 132003 (2013); F. K. Guo, C. H. Duque, and J. Nieves, Phys. Rev. D **88**, 054007 (2013); J. R. Zhang, Phys. Rev. D **87**, 116004 (2013); Y. B. Dong, A. Faessler, T. Gutsche, and V. E. Lyubovitskij, Phys. Rev. D **88**, 014030 (2013); E. Wilbring, H. W. Hammer, and U. G. Meißner, Phys. Lett. B **726**, 326 (2013); W. Chen, T. G. Steele, M. L. Du, and S. L. Zhu, Eur. Phys. J. C **74**, 2773 (2014); J. He, X. Liu, Z. F. Sun, and S. L. Zhu, Eur. Phys. J. C **73**, 2635 (2013); H. W. Ke, Z. T. We, and X. Q. Li, Eur. Phys. J. C **73**, 2561 (2013).

[11] L. Maiani, V. Riquer, R. Faccini, F. Piccinini, A. Pilloni, and A. D. Polosa, Phys. Rev. D **87**, 111102 (2013); J. M. Dias, F. S. Navarra, M. Nielsen, and C. M. Zanetti, Phys. Rev. D **88**, 016004 (2013); E. Braaten, Phys. Rev. Lett. **111**, 162003 (2013); C. F. Qiao and L. Tang, arXiv:1307.6654v1; Eur. Phys. J. C **74**, 2810 (2014); Z. G. Wang and T. Huang, Phys. Rev. D **89**, 054019 (2014); Z. G. Wang, arXiv:1312.1537v2.

[12] I. V. Danilkin, V. D. Orlovsky, and Y. A. Simonov, Phys. Rev. D **85**, 034012 (2012); N. Mahajan, arXiv:1304.1301.

[13] M. B. Voloshin, Phys. Rev. D **87**, 091501 (2013).

[14] C. R. Deng, J. L. Ping, F. Wang, and T. Goldman, Phys. Rev. D **82**, 074001 (2010).

[15] C. R. Deng, J. L. Ping, H. Wang, P. Zhou, and F. Wang, Phys. Rev. D **86**, 114035 (2012).

[16] C. R. Deng, J. L. Ping, Y. C. Yang, and F.Wang, Phys. Rev. D **86**, 014008 (2012).

[17] C. R. Deng, J. L. Ping, Y. C. Yang, and F.Wang, Phys. Rev. D **88**, 074007 (2013).

[18] C. R. Deng, J. L. Ping, P. Zhou, and F. Wang, Chin. Phys. C **37**, 033101 (2013).

[19] N. Isgur and G. Karl, Phys. Rev. D **18**, 4187 (1978); **19**, 2653 (1979); **20**, 1191 (1979).

[20] Y. Fujiwara, C. Nakamoto, and Y. Suzuki, Phys. Rev. C **54**, 2180 (1996); Y. Fujiwara, M. Khono, C. Nakamoto, and Y. Suzuki, Phys. Rev. C **64**, 054001 (2001); Y. Fujiwara, K. Miyagawa, M. Khono, Y. Suzuki, and C. Nakamoto, Nucl. Phys. **A737**, 243 (2004).

[21] J. Weinstein and N. Isgur, Phys. Rev. Lett. **48**, 659 (1982); M. Oka, Phys. Rev. D **31**, 2274 (1985); M. Oka and C. J. Horowitz, Phys. Rev. D **31**, 2773 (1985).

[22] V. Dmitrasinovic, Phys. Rev. D **67**, 114007 (2003).
[23] D. Robson, Phys. Rev. D **35**, 1018 (1987).
[24] C. Alexandrou, P. D. Forcrand, and A. Tsapalis, Phys. Rev. D **65**, 054503 (2002); T. T. Takahashi, H. Suganuma, Y. Nemoto, and H. Matsufuru, Phys. Rev. D **65**, 114509 (2002); F. Okiharu, H. Suganuma, and T. T. Takahashi, Phys. Rev. Lett. **94**, 192001 (2005).
[25] F. Okiharu, H. Suganuma, and T. T. Takahashi, Phys. Rev. D **72**, 014505 (2005).
[26] J. L. Ping, C. R. Deng, F. Wang, and T. Goldman, Phys. Lett. B **659**, 607 (2008).
[27] F. Wang and C. W. Wong, Nuovo Cimento Soc. Ital. Fis. **86A**, 283 (1985).
[28] T. Goldman and S. Yankielowicz, Phys. Rev. D **12**, 2910 (1975).
[29] R. L. Jaffe and F. Wilczek, Phys. Rev. Lett. **91**, 232003 (2003); R. L. Jaffe, Phys. Rep. **409**, 1 (2005).
[30] G. S. Bail, Phys. Rev. D **62**, 114503 (2000); C. Semay, Eur. Phys. J. A **22**, 353 (2004); N. Cardoso, M. Cardoso, and P. Bicudo, Phys. Lett. B **710**, 343 (2012).
[31] J. Vijande, F. Fernandez, and A. Valcarce, J. Phys. G **31**, 481 (2005).
[32] J. Weinstein and N. Isgur, Phys. Rev. D **27**, 588 (1983).
[33] J. Vijande, E. Weissman, A. Valcarce, and N. Barnea, Phys. Rev. D **76**, 094027 (2007); J. Vijande, E. Weissman, N. Barnea, and A. Valcarce, Phys. Rev. D **76**, 094022 (2007).
[34] E. Santopinto and G. Galatà, Phys. Rev. C **75**, 045206 (2007).
[35] E. A. G. Armoura, J. M. Richard, and K. Varga, Phys. Rep. **413**, 1 (2005).
[36] J. P. Ader, J. M. Richard, and P. Taxil, Phys. Rev. D **25**, 2370 (1982); L. Heller and J. A. Tjon, Phys. Rev. D **35**, 969 (1987).
[37] E. Hiyama, Y. Kino, and M. Kamimura, Prog. Part. Nucl. Phys. **51**, 223 (2003).
[38] E. Eichten, K. Gottfried, T. Kinoshita, J. Kogut, K. D. Lane, and T. M. Yang, Phys. Rev. Lett. **34**, 369 (1975).
[39] S. Godfrey and N. Isgur, Phys. Rev. D **32**, 189 (1985).
[40] M. D. Scadron, Phys. Rev. D **26**, 239 (1982).
[41] M. Chen, H. X. Huang, J. L. Ping, and F. Wang, Phys. Rev. C **83**, 015202 (2011); H. X. Huang, J. L. Ping, and F. Wang, Phys. Rev. C **89**, 035201 (2014); J. Vijande, F. Fernández, A. Valcarce1, and B. Silvestre-Brac, Eur. Phys. J. A **19**, 383 (2004).
[42] J. Vijande, A. Valcarce, and J. M. Richard, Phys. Rev. D **76**, 114013 (2007).
[43] Y. C. Yang, C. R. Deng, J. L. Ping, and T. Goldman, Phys. Rev. D **80**, 114023 (2009).
[44] D. Ebert, R. N. Faustov, and V. O. Galkin, Phys. Lett. B **634**, 214 (2006).
[45] D. Y. Chen, X. Liu, and T. Matsuki, Phys. Rev. Lett. **110**, 232001 (2013).
[46] Y. C. Yang, J. L. Ping, C. R. Deng, and H. S. Zong, J. Phys. G **39**, 105001 (2012).
[47] J. Carlson, L. Heller, and J. A. Tjon, Phys. Rev. D **37**, 744 (1988); H. J. Lipkin, Phys. Lett. B **172**, 242 (1986).
[48] F. Wang, J. L. Ping, H. R. Pang, and L. Z. Chen, Nucl. Phys. **A790**, 493c (2007).
[49] S. Weinberg, *The Quantum Theory of Fields*, (Cambridge University Press, Cambridge, England, 1995), Vol. I, p. 159.